HMGB-1 induces c-kit$^+$ cell microvascular rolling and adhesion *via* both toll-like receptor-2 and toll-like receptor-4 of endothelial cells

Dario Furlani [a, #], Peter Donndorf [a, #], Ingeborg Westien [a], Murat Ugurlucan [a], Erik Pittermann [a], Weiwei Wang [a, b], Wenzhong Li [a, c, *, #], Brigitte Vollmar [d], Gustav Steinhoff [a, ‡], Alexander Kaminski [a, #], Nan Ma [a, b, *, #]

[a] Reference and Translation Centre for Cardiac Stem Cell Therapy (RTC), Department of Cardiac Surgery, University Rostock, Rostock, Germany
[b] Centre for Biomaterial Development, Institute of Polymer Research, Helmholtz-Zentrums Geesthacht, Teltow, Germany
[c] Berlin-Brandenburg Center for Regenerative Therapies, Charité – Universitätsmedizin, Berlin, Germany
[d] Institute for Experimental Surgery, University of Rostock, Rostock, Germany

Abstract

High-mobility group box 1 (HMGB-1) is a strong chemo-attractive signal for both inflammatory and stem cells. The aim of this study is to evaluate the mechanisms regulating HMGB-1–mediated adhesion and rolling of c-kit$^+$ cells and assess whether toll-like receptor-2 (TLR-2) and toll-like receptor-4 (TLR-4) of endothelial cells or c-kit$^+$ cells are implicated in the activation of downstream migration signals to peripheral c-kit$^+$ cells. Effects of HMGB-1 on the c-kit$^+$ cells/endothelial interaction were evaluated by a cremaster muscle model in wild-type (WT), TLR-2 ($-/-$) and Tlr4 (LPS-del) mice. The mRNA and protein expression levels of endothelial nitric oxide synthase were determined by quantitative real-time PCR and immunofluorescence staining. Induction of crucial adhesion molecules for rolling and adhesion of stem cells and leukocytes were monitored *in vivo* and *in vitro*. Following local HMGB-1 administration, a significant increase in cell rolling was detected (32.4 $\pm$ 7.1% in 'WT' *versus* 9.9 $\pm$ 3.2% in 'control', $P < 0.05$). The number of firmly adherent c-kit$^+$ cells was more than 13-fold higher than that of the control group (14.6 $\pm$ 5.1 cells/mm^2 in 'WT' *versus* 1.1 $\pm$ 1.0 cells/mm^2 in 'control', $P < 0.05$). In knock-out animals, the fraction of rolling cells did not differ significantly from control levels. Firm endothelial adhesion was significantly reduced in TLR-2 ($-/-$) and Tlr4 (LPS-del) mice compared to WT mice (1.5 $\pm$ 1.4 cells/mm^2 in 'TLR-2 ($-/-$)' and 2.4 $\pm$ 1.4 cells/mm^2 in 'Tlr4 (LPS-del)' *versus* 14.6 $\pm$ 5.1 cells/mm^2 in 'WT', $P < 0.05$). TLR-2 ($-/-$) and Tlr4 (LPS-del) stem cells in WT mice did not show significant reduction in rolling and adhesion compared to WT cells. HMGB-1 mediates c-kit$^+$ cell recruitment *via* endothelial TLR-2 and TLR-4.

Keywords: high-mobility group box 1 • c-kit$^+$ • intravital microscopy • cremaster muscle

Introduction

The importance of chemokines and local inflammation for stem cell trafficking to injured tissue has been shown in the recent past

[1]. HMGB-1, also called ampthotericin, is a highly conserved, ubiquitously expressed, nuclear protein [2], which is released in the extracellular space by necrotic but not apoptotic cells. Moreover, HMGB-1 is secreted by cells after inflammatory activation and acts in the extracellular space as a chemoattractant for inflammatory cells, smooth muscle cells and stem cells [3, 4]. The receptor for advanced glycation end-products (RAGE) and members of the TLR family are known cellular receptors of HMGB-1. Recently, HMGB-1 has been shown to enhance integrin-dependent homing of endothelial progenitor cells [5]. HMGB-1 is also capable to induce mesoangioblast migration through an endothelial

[#]These authors contributed equally to this work.
*Correspondence to: Dr. Nan MA and Dr. Wenzhong LI,
Reference and Translation Center for Cardiac Stem Cell Therapy (RTC),
Department of Cardiac Surgery, University Rostock,
Schillingallee 69, 18057 Rostock, Germany.
Tel.: +49-381-494 6105
Fax: +49-381-494 6214
E-mail: nan.ma@med.uni-rostock.de; wenzhong.li@med.uni-rostock.de

monolayer *in vitro*, and may act *in vivo* as a signal to attract both mesoangioblast and bone marrow derived stem cells [6]. On the other hand, HMGB-1 in endothelial cells induces the up-regulation of adhesion molecules VCAM-1 and ICAM-1, which are required for integrin-mediated adhesion and subsequent transmigration of inflammatory cells [7]. Stem cell adhesion and homing relay on similar mechanisms. Bone marrow derived stem cells and endothelial progenitor cells require β1-integrin and β2-integrin for their transmigration through the endothelial barrier [8]. In a murine model of myocardial infarction, exogenously administrated HMGB-1 led to recovery of left ventricular function through regeneration of cardiomyocytes from resident cardiac c-kit$^+$ stem cells [9], suggesting that the presence HMGB-1 may have physiological relevance in the setting of ischaemic cardiovascular pathologies.

C-kit, as a murine hemangioblast marker, is continued to be expressed in their adulthood [10]. These cells, including endothelial progenitor cell (EPC) and haematopoietic stem cell (HSC), have been implicated in contributing to angiogenesis, organ repair and tissue remodelling by migrating from the bone marrow into the peripheral circulation. Therefore, it is highly important to examine c-kit$^+$ cell rolling and adhesion in the microvascular endothelium [11, 12].

In this study, we aimed to investigate HMGB-1 ability to regulate c-kit$^+$ cell–endothelium interactions in the cremaster muscle microcirculation, using intravital fluorescence microscopy. We found that HMGB-1–mediated peripheral c-kit$^+$ cell recruitment did not depend on the presence of TLRs 2 or 4 of stem cells but depended on both, TLR-2 and TLR-4 of endothelial cells. In addition, we evaluated whether HMGB-1 affects adhesion molecule redistribution in endothelial cells *in vitro*.

Materials and methods

Experimental design

All animal experiments were carried out according to the Guide for the Care and Use of Laboratory Animals (NIH Publication No. 85–23, revised 1996) and were permitted by the local animal care and use committee. Lipopolysaccharide (LPS, Endotoxin), representing a known pro-inflammatory molecule and TLR-4 agonist, was obtained from Sigma-Aldrich (Munich, Germany). The macrophage-activating lipopeptide 2 kD (MALP-2), representing a selective TLR-2 agonist, was obtained from Enzo Life Sciences (L˘rrach, Germany). Male WT mice (C57BL/6J, Charles River, Sulzfeld, Germany) weighing 20–25 g were stochastically selected as bone marrow donors for *in vitro* ($n = 10$) and *in vivo* ($n = 50$) experiments or as recipient for cell injection and intravital fluorescence microscopy analysis ($n = 48$). TLR-2 ($-/-$) (B6.129-Tlr2Tm1kir/j) ($n = 12$) and Tlr4 (LPS-del) (C3H/HeJ) mice ($n = 12$) (Charles River) were assigned to intravital fluorescence microscopy analysis ($n = 6$) and to bone marrow donation ($n = 6$). The WT mice underwent surgical procedure (cremaster muscle preparation) and topical administration of 200 μl of HMGB-1 (HMGBiotech, Turin, Italy; 400 ng/ml in PBS; 'HMGB-1' group; $n = 10$), 200 μl of heated HMGB-1 (HMGBiotech; 400 ng/ml in PBS; boiled for 15 min.; 'Control' group; $n = 11$), LPS (50 ng/kg in PBS; 'LPS' group; $n = 4$) or MALP-2 (1.25 μg/ml in PBS; 'MALP-2' group; $n = 4$). TLR-2

($-/-$) and Tlr4 (LPS-del) mice were operated with the same procedure used for WT and were topically treated with HMGB-1 (400 ng/ml in PBS; HMGBiotech, 'TLR-2ko' group, $n = 6$; 'TLR-4ko' group, $n = 6$). WT mice were randomly chosen as recipients for TLR-2 ($-/-$) and Tlr4 (LPS-del) c-kit$^+$ cell injection ('TLR-2ko cell' group, $n = 6$; 'TLR-4ko cell' group, $n = 6$). HMGB-1 stimulated cell migration in a concentration-dependent manner [6, 13]. Following intravital microscopic analysis, mice were killed and their cremaster muscles were collected and cut in two parts. One half of the muscle was fixed in 4% formaldehyde and embedded in paraffin for histological examination; the other half was snap-frozen in liquid nitrogen for real-time PCR analysis.

To provide similar microcirculatory conditions within the experimental groups, several parameters were measured and taken into careful consideration. Red blood cell velocity profile was verified using the line shift method on intravital microscopy recordings (CapImage Software, Zeintl, Heidelberg, Germany). The analyses of microcirculation also included the measurement of vessel diameter and wall shear rates based on the Newtonian definition $\gamma = 8 \times v/d$, where '*v*' represents the red blood cell velocity divided by 1.6 according to the Baker-Wayland factor [14] and '*d*' represents the single vessel diameter (Table S1).

Intravital fluorescence microscopy: c-kit+ cell behaviour at the interface of venular endothelium following HMGB-1 stimulus

Male WT mice, TLR-2 ($-/-$) mice and Tlr4 (LPS-del) were anaesthetized with ketamine (75 mg/kg) and xylazine (25 mg/kg). An arterial catheter was inserted retrograde into the left femoral artery to establish the injection route for fluorescent reagents and labelled c-kit$^+$ cells. The right cremaster muscle was dissected and prepared for intravital fluorescence microscopic analysis as previously described [15, 16]. For intravital microscopy, c-kit$^+$ and c-kit$^+$ TLR-2 ($-/-$) and Tlr4 (LPS-del) cells were fluorescently labelled with the CFDA SE (carboxy-fluorescein diacetate, succinimidyl ester; A2 Molecular Probes, Carlsbad, CA) according to manufacturer's protocol. To observe the inflammatory response to HMGB-1, circulating endogenous leukocytes (ELs) of recipient origin were coloured by intravenous injection of 0.1 ml of 1% rhodamine 6G (Sigma-Aldrich). Fluorescently-labelled dextran was injected to visualize the blood flow. Rhodamine 6G (background for CFDA SE-labelled c-kit$^+$ cells) or fluorescein isothiocyanate (background for rhodamine-labelled EL) were used as background. As intravital microscopy system, an Axiotech fluorescence microscope (Carl Zeiss, Jena, Germany) was modified for epi-illumination and connected to a charge-coupled device (CCD) video camera. Six post-capillary venules were randomly chosen before cell injection to define the areas of cellular adherence analysis. With respect to the groups, the cremaster muscles were exposed to HMGB-1, heated HMGB-1, LPS or MALP-2, 15 min. before the first c-kit$^+$ cell injection. In 'HMGB-1' and 'Control' groups, CFDA SE–labelled c-kit$^+$, c-kit$^+$ TLR-2 ($-/-$) or Tlr4 (LPS-del) cells were applied at 0.4×10^6 cells per injection, with a total of five consecutive injections. In 'LPS' and 'MALP-2' groups, only WT c-kit$^+$ cells were injected. C-kit$^+$ cell behaviour along the endothelial lining was considered as 'rolling' when a more than 50% reduction of cell velocity in combination with the typical cellular 'stick and release' motion was present. The rolling cells were expressed as percentage of all passing cells along a predefined venular distance during 1 min. of observation. All the cells that showed random brief tethering phenomena were not considered as rolling cells. Firm

adhesion was recorded when cells did not move for more than 30 sec. The number of firmly adherent c-kit$^+$ cells was calculated in relation to the endothelial surface of the predefined venules (diameter $\times$ length $\times$ π) and was expressed as adherent cells/mm^2 endothelial surface. Intravital fluorescence microscopy analysis was carried out by two researchers, who were blinded to the treatment.

Quantitative real-time PCR analysis

For analysis of mRNA levels, cremaster muscles ($n = 6$, for each group) were removed and carefully dissected along the central axis. The two half were separated and one of them was snap-frozen in liquid nitrogen. Total RNA was extracted following the instructions of the TRIZOL$^®$ Reagent (Invitrogen, Carlsbad, CA, USA) including DNase treatment. Primer sets for real-time PCR (Applied Biosystems, Foster City, CA, USA) are summarized in Table S2. Amplification and detection were carried out with the StepOnePlus™Real-Time PCR System (Applied Biosystems) in TaqMan Universal Master Mix (Applied Biosystems), according to the instructions of the producer (Applied Biosystems). Reactions were repeated at least three times using the following program: 1 cycle of 50°C for 2 min., 1 cycle of 95°C for 10 min. and 40 cycles of 95°C for 15 sec. and 60°C for 1 min. DNA extracts were analysed in at least triplicate and negative controls were included in each assay. Cycle thresholds (C_T) for individual reactions were determined with StepOne™ Software 2.0 (Applied Biosystems) and the target genes were normalized against GAPDH with the formula: $\Delta C_T = C_{T \text{ target}} - C_{T \text{ GAPDH}}$. Calculated ΔC_T of triplicates was averaged and $\Delta \Delta C_T$ were obtained using 'Control' group as calibrator sample (formula: $\Delta \Delta C_T = \Delta C_{T \text{ sample}} - \Delta C_{T \text{ calibrator sample}}$). The changes in gene expression after HMGB-1 treatment were expressed as fold differences ($2^{-\Delta \Delta C}$).

Immunohistochemistry

After sacrifice of recipients, the cremaster muscles were removed and divided in two pieces for downstream analyses. From these, one piece was fixed in 4% formaldehyde and embedded in paraffin for immunohistochemistry (at least $n = 5$, for each group). After deparaffinization and protein retrieving, cremaster tissue sections (5 μm thick) were incubated with mouse antimouse endothelial nitric oxide synthase (eNOS) monoclonal antibody overnight (Becton Dickinson, Heidelberg, Germany). On the second day, an Alexa 488 conjugated donkey antimouse secondary antibody (Molecular Probes) was applied on the sections. TOPRO 3 (Invitrogen) was used to label the nuclei. Following fluorescent staining, the tissue was analysed by TCS SPE confocal microscopy (Leica Microsystems). Observations were performed by one investigator, who was blinded to the treatment.

Isolation and fluorescent-activated cell sorter analysis of c-kit$^+$ cells from murine bone marrow

c-kit$^+$ cells were isolated from mouse (C57BL/6J; B6.129-Tlr2Tm1kir/j and C3H/HeJ; 8 weeks old) bone marrow using magnetic microbeads coated with anti–c-kit monoclonal antibody, Miltenyi Biotec MS columns$^®$ and the MiniMacs$^®$ cell separation system (Miltenyi Biotec, Bergisch

Gladbach, Germany). Cell separation cycle was repeated two times to obtain higher cell number. To perform flow cytometry analysis, cells were incubated for 10 min. at 4°C with monoclonal antimouse CD117 conjugated with PE (clone 3C1; 1:10; Miltenyi Biotec, Bergisch Gladbach, Germany), mouse antimouse TLR-2 antibody (Santa Cruz, Santa Cruz, CA, USA) and goat antimouse TLR-4 antibody (Abcam, Cambridge, MA, USA). After primary antibody reaction, cells were washed and resuspended with antimouse and anti-goat Alexa 488 secondary antibodies (Invitrogen). Cells were washed with phosphate-buffered saline (PBS)/2 mM EDTA and analysed by an FACS LSR II flow cytometer (Becton Dickinson). Dead cells were excluded with propidium iodide staining. Analysis of data was carried out with BD FACS Diva software. At least 10,000 events per sample were recorded to create side scatters plots against logarithmic fluorescence intensity. The purity of the enriched c-kit$^+$ cell preparation tested with flow cytometry was consistently higher than 95% (Fig. S1).

Immunofluorescence analysis of β1-integrin, P-selectin and ICAM-1 motility on SVEC membrane following HMGB-1 preconditioning

It has been shown that HMGB receptor is present on microvascular endothelial cells [7]. To investigate endothelial activation mediated by HMGB-1 mouse endothelial cells (SVEC) were pre-treated with the chemokine to induce a prompt cellular response with an increase of adhesion molecule valency/avidity. The increased proteins affinity and membrane redistribution might be implicated in the cellular migratory activity. HMGB-1 effect was compared with activities of other well-known chemokines such as TNF-α and stromal derived factor 1α (SDF-1α).

To mimic the endothelial response to HMGB-1 *in vitro*, simian virus 40-transformed mouse endothelial cell (SVEC) were incubated in the presence of active or heated HMGB-1 (100 ng/ml). Tumour necrosis factor α (TNF-α; 200 U/ml; R&D Systems, Minneapolis, MN, USA) or SDF-1α (100 ng/ml; R&D Systems) were utilized as positive controls. Slides preparation and P-selectin staining were obtained utilizing the protocols previously described used for c-kit$^+$ cells. For β1-integrin and ICAM-1 detection, hamster antimouse β1-integrin monoclonal, hamster antimouse ICAM-1 antibodies (Becton Dickinson) and a goat anti-hamster Alexa 488 conjugated secondary antibody (Molecular Probes) were utilized in sequence. Nuclei were detected by TOPRO 3 counterstain (Invitrogen) and probes were investigated with TCS SPE confocal microscopy (Leica Microsystems). The numbers of SVEC cells presenting β-integrin, P-selectin or ICAM-1 polarization were counted in 20 randomly chosen high-power fields (HPFs, 630$\times$). Results were expressed as cells per HPF. All morphometric analyses were performed by two investigators who were blinded to the treatment.

Statistical analyses

All statistical analyses were performed using Sigma Stat software version 3.0 (SPSS Inc., Chicago, IL, USA). Results are showed as mean $\pm$ S.E.M. Comparisons of the groups were executed using the one-way ANOVA, which applies *post-hoc* multiple Holm–Sidak analysis. In case the data failed normality testing, the non-parametric Kruskal–Wallis or *post-hoc* multiple Dunn tests were employed. $P < 0.05$ was considered statistically significant.
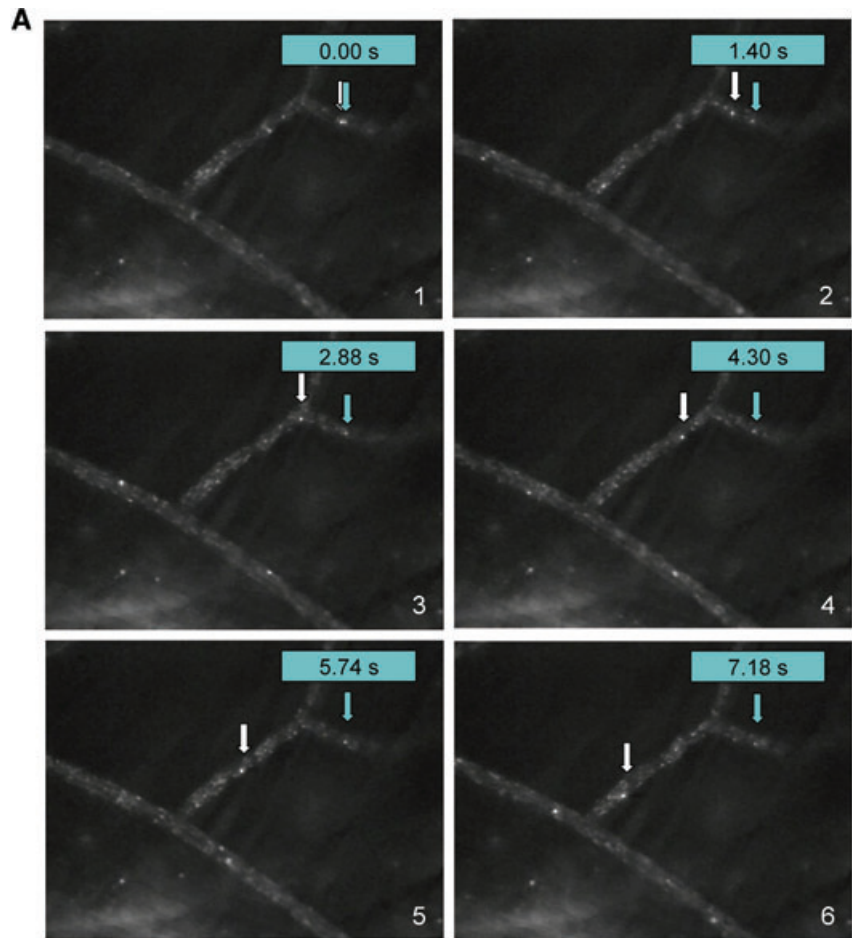
Fig. 1 Effects of direct HMGB-1 superfusion of cremaster muscle on c-kit$^+$ cell rolling and adhesion 15 min. after treatment. (**A**) Representative intravital fluorescence microscopy images of rolling and adherent c-kit$^+$ cells. (**B**) Percentage of rolling c-kit$^+$ cells in 'Control', 'HMGB-1', 'LPS' and 'MALP-2' groups. (**C**) Amount of adherent c-kit$^+$ cells in 'Control', 'HMGB-1', 'LPS' and 'MALP-2' groups (*$P < 0.05$ *versus* 'Control', #$P < 0.05$ *versus* 'HMGB-1').
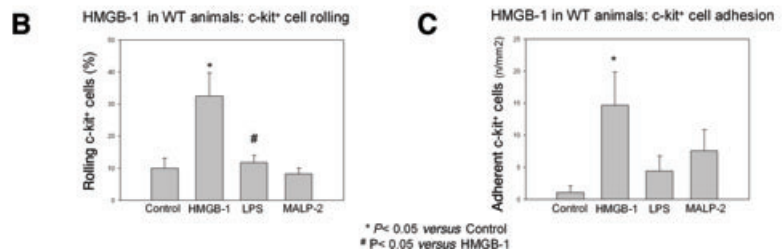
Results

In vivo interaction of c-kit$^+$ cells with the endothelium was predominant in post-capillary venules

Overall, interaction between injected c-kit$^+$ cells and the vascular endothelium was a rare event and occurred almost exclusively in post-capillary venules (diameter: 40–80 μm). c-kit$^+$ cell contact to endothelial lining arised to a different extent in the respective experimental groups. In the observed venules, rolling and firmly adherent c-kit$^+$ cells in response to superfusion of HMGB-1 could be clearly counted (Fig. 1A).

HMGB-1 alone enhances venular rolling of c-kit$^+$ cells *in vivo*

In vivo rolling c-kit$^+$ cells were quantified using intravital fluorescence microscopy. There was a more than 50% reduction of

velocity along the endothelial lining. In the heated HMGB-1-superfused cremaster muscle ('Control'), the fraction of rolling c-kit^{+} cells was 9.9 ± 3.2%. Following local HMGB-1 administration, a more than three-fold increase in c-kit[+] cell rolling was detected (32.4 ± 7.1% in 'HMGB-1' versus 9.9 ± 3.2% in 'Control', $P < 0.05$; Fig. 1B). Additional local treatment with SDF-1α had no further impact on the percentage of rolling c-kit^{+} cells (data not shown).

LPS and MALP-2 did not lead to significant rolling of c-kit^{+} cells

To clarify the effect of TLR-2 and TLR-4 on c-kit[+] cell rolling after specific activation, we treated the cremaster muscle either with LPS or MALP-2. Intravital microscopy data did not show a significant variation of cellular rolling in 'LPS' and 'MALP-2' groups when compared to 'Control'(c-kit[+] cell rolling: 11.8 ± 2.3% in 'LPS' and 8.1 ± 2.0% in 'MALP-2' versus 9.9 ± 3.2% in 'Control', $P = 0.37$; Fig. 1B).

HMGB-1 enhances firm endothelial adhesion of c-kit^{+} cells *in vivo*

The number of firmly adherent c-kit^{+} cells after cremaster muscle superfusion with heated HMGB-1 ('Control') was 1.1 ± 1.0 cells/mm^{2}. In response to treatment with the active chemokine, the number of firmly adherent c-kit^{+} cells was significantly higher than in respective control group (c-kit[+] cell adhesion: 14.6 ± 5.1 cells/mm^{2} in 'HMGB-1' versus 1.1 ± 1.0 cells/mm^{2} in 'Control', $P < 0.05$). In fact, stem cell adhesion after tissue stimulation with HMGB-1 exceeded that of the untreated control mice more than 13-fold (Fig. 1C). Once more, after combined treatment of the cremaster muscle tissue with HMGB-1 and SDF-1α, the number of adherent c-kit^{+} cells was not further enhanced (data not shown).

LPS and MALP-2 induce moderate adhesion of c-kit^{+} cells

We tested whether TLR-2 and TLR-4 targeted stimulation on the cremaster muscle could influence c-kit[+] cell adhesion. Following topical administration of LPS or MALP-2, we observed by intravital microscopy an increase of c-kit[+] cell adhesion in 'LPS' and 'MALP-2' groups when compared to 'Control' (c-kit[+] cell adhesion: 4.4 ± 2.3 cells/mm^{2} in 'LPS' and 7.5 ± 3.3 cells/mm^{2} in 'MALP-2' versus 1.1 ± 1.0 cells/mm^{2} in 'Control', $P = 0.27$; Fig. 1C). However, the levels of adherent cells in these groups were not comparable with the amount of firm adhesion observed in 'HMGB-1' group.

HMGB did not induce WT c-kit rolling and firm adhesion in TLR-2 and TLR-4 knockout mice

To further validate the role of TLR-2 and TLR-4 in HMGB-1–mediated endothelial adhesion behaviour of c-kit^{+} cells, we studied stem cell endothelial interactions in TLR-2 (−/−) and Tlr4 (LPS-del) mice, after HMGB-1 stimulation *in vivo.* The fraction of rolling cells did not differ significantly from wild-type control levels in TLR-2 (−/−) and Tlr4 (LPS-del) mice after local treatment with HMGB-1 (c-kit[+] cell rolling: 8.8 ± 3.9% in 'TLR-2ko' and 3.1 ± 1.6% in 'TLR-4ko' versus 9 ± 3.2% in 'Control', $P = 0.3$). In contrast to WT mice, the local treatment with HMGB-1 in TLR-2 (−/−) and Tlr4 (LPS-del) did not induce rolling (Fig. 2A). The number of firmly adherent c-kit^{+} cells was clearly reduced in TLR-2 (−/−) and Tlr4 (LPS-del) animals after local treatment with HMGB-1 compared to WT mice after HMGB-1 stimulation (c-kit cell adhesion: 1.5 ± 1.4 cells/mm^{2} in 'TLR-2ko' and 2.4 ± 1.4 cells/mm^{2} in 'TLR-4ko' versus 14.6 ± 5.1 cells/mm^{2} in 'HMGB-1', $P < 0.05$; Fig. 2B). It is reasonable to speculate HMGB-1 mediates c-kit[+] cell recruitment *via* both the TLR-2 and TLR-4 signalling of endothelial cells.

HMGB induces rolling and firm adhesion of c-kit^{+} cells from TLR-2 and TLR-4 knockout in WT microvasculature

Because TLR is presented on both endothelial cell and stem cell surface, it is important to clarify whether the reported effect of HMGB-1 on c-kit[+] cell–endothelial cell interaction is additionally mediated *via* TLR on the stem cell side. We, therefore, investigated rolling and adhesion capacity of c-kit^{+} cells from TLR-2 and TLR-4 knockout mouse in WT microvasculature. HMGB-1 induces rigorous cell migration. The number of rolling TLR-2 (−/−) c-kit[+] and Tlr4 (LPS-del) c-kit^{+} cells was significantly increased compared to untreated 'Control' (c-kit[+] cell rolling: 18.6 ± 1.2% in 'TLR-2ko cell' and 18.2 ± 2.2% in 'TLR-4ko cell' versus 9 ± 3.2% in 'Control', $P < 0.01$ and $P < 0.05$). There was no significant difference on rolling cell number in 'TLR-2ko cell' and 'TLR-4ko cell' groups compared to 'HMGB-1'group (Fig. 2C). The number of firmly adherent TLR-2 (−/−) and Tlr4 (LPS-del) c-kit^{+} cells was significantly increased after topical HMGB-1 application compared to 'Control' mice (c-kit[+] cell adhesion: 16.3 ± 5.2 cells/mm^{2} in 'TLR-2ko cell' and 11.7 ± 3.6 cells/mm^{2} in 'TLR-4ko cell' versus 1.1 ± 1.0 cells/mm^{2} in 'Control', $P < 0.05$; Fig. 2D). There was no significant difference on adherent cell number in 'TLR-2ko cell' and 'TLR-4ko cell' groups compared to 'HMGB-1'group ($P = 0.84$ and 0.82, respectively). This data suggest that mobilization and recruitment of c-kit[+] cell by HMGB-1 do not require the presence of TLR-2/4 on c-kit[+] cell membrane.

HMGB-1 mediated up-regulation of eNOS and c-kit expression is TLR-2 dependent

We examined whether HMGB-1 treatment altered eNOS and c-kit expression in the cremaster muscle by real-time PCR and

Fig. 2 HMGB-1–mediated c-kit[+] cell rolling and adhesion on cremaster muscle. (**A**) Percentage of rolling WT c-kit^{+} cells in TLRs knockout mice. (**B**) Quantity of adherent WT c-kit^{+} cells in TLRs knockout mice. (**C**) Percentage of rolling TLR-2 (−/−) and Tlr4 (LPS-del)c-kit^{+} cells in WT animals. (**D**) Number of adherent TLR-2 (−/−) and Tlr4 (LPS-del) c-kit^{+} cells in WT animals (*$P < 0.05$ *versus* 'Control', **$P < 0.01$ *versus* 'Control', #$P < 0.05$ *versus* 'HMGB-1').
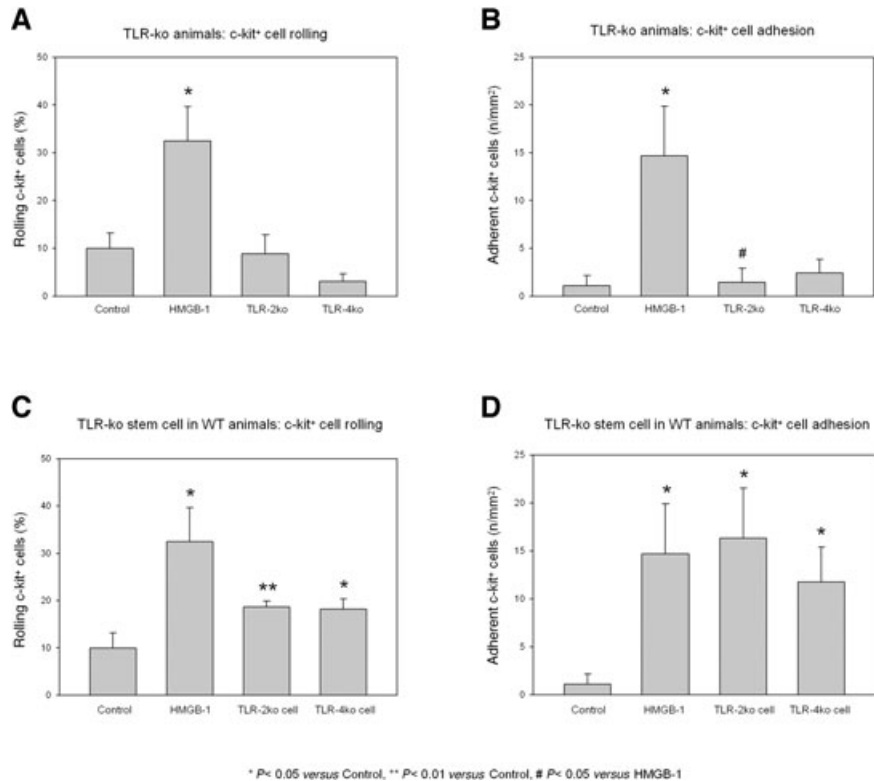
immunostaining. Quantitative real-time PCR revealed that eNOS mRNA was significantly up-regulated in HMGB-1 superfused muscles ($P < 0.05$; Fig. 3A) compared with 'Control'. These data were further supported by immunostaining of eNOS, which identified a clear eNOS expression pattern in HMGB-1–treated cremaster muscles: eNOS was detected in the endothelial cells bordering the vessel lumen (Fig. 3B). Furthermore, the mRNA level of c-kit was considerably increased after HMGB-1 superfusion compared to the heated chemokine (Fig. 3A).

To uncover the role of TLRs in HMGB-1–mediated c-kit[+] cell interaction with the endothelium, we verified eNOS and c-kit mRNA expression in the knockout animals ('TLR-2ko' and 'TLR-4ko' groups). Interestingly, the lack of TLR-2 abolished completely the positive regulation of eNOS and c-kit triggered by HMGB-1 (Fig. 3A). In the absence of TLR-4, there was no significant change of the two genes compared to 'HMGB-1' ($P > 0.05$; Fig. 3A).

HMGB-1–mediated up-regulation of P-selectin expression is TLR-2 dependent

To clarify the effects of HMGB-1 on the adhesion capacity of endothelial and circulating cells, quantitative real-time PCR was performed and mRNA levels of P-selectin were quantified. As

shown in Figure 4, the mRNA level of P-selectin was up-regulated in response to HMGB-1 cremaster superfusion ($P < 0.01$). Thus, cell adhesive properties were promptly increased after local HMGB-1 application. In the TLR-2 knockout mice, P-selectin expression was drastically down-regulated ($P < 0.01$; Fig. 4), suggesting a crucial role of the receptor in HMGB-1–mediated cell adhesion competence.

Inflammatory response after low-dosage HMGB-1 superfusion of the cremaster muscle

Given the potential role of HMGB-1 as mediator of inflammatory response, we carefully evaluated the feasible dosage of the chemokine (dose/response test) by intravital fluorescence microscopy (data not shown). After choosing the favourable amount of protein (400 ng/ml), the expression of crucial markers of inflammation such as β1-integrin and leukocyte common marker CD45 was assessed by real-time PCR. HMGB-1 superfusion induced a moderate increase in EL adhesion (Fig. 5A). However, the levels of β1-integrin and CD45 mRNAs did not change significantly in response to HMGB-1 signal (Fig. 5B). In 'TLR-2ko' group, expression levels of the two analysed mRNAs were significantly reduced (Fig. 5B).
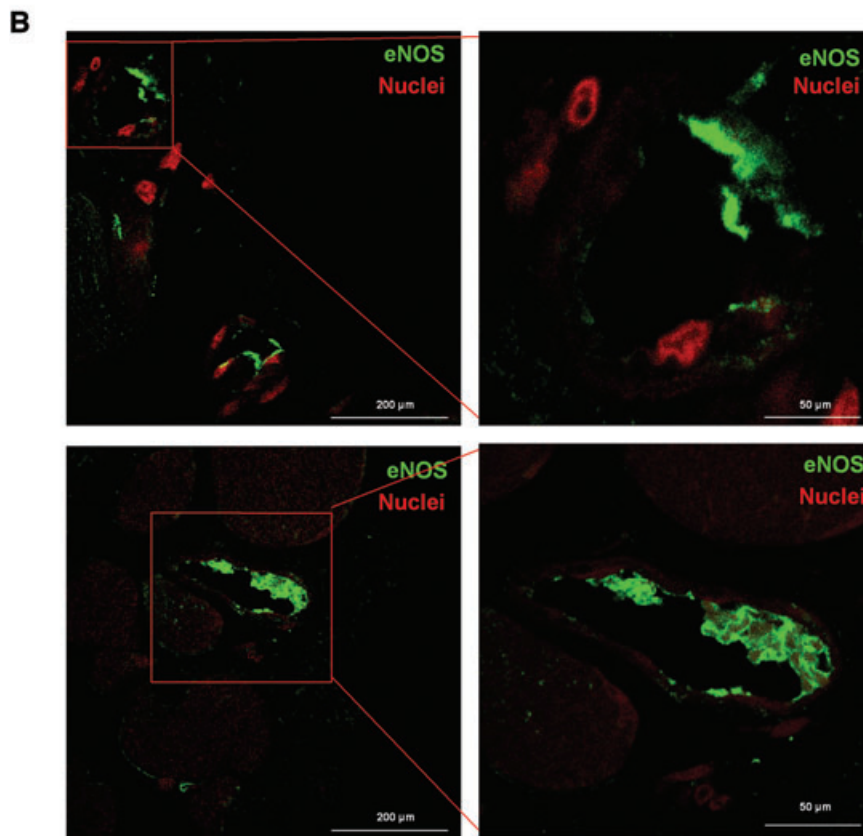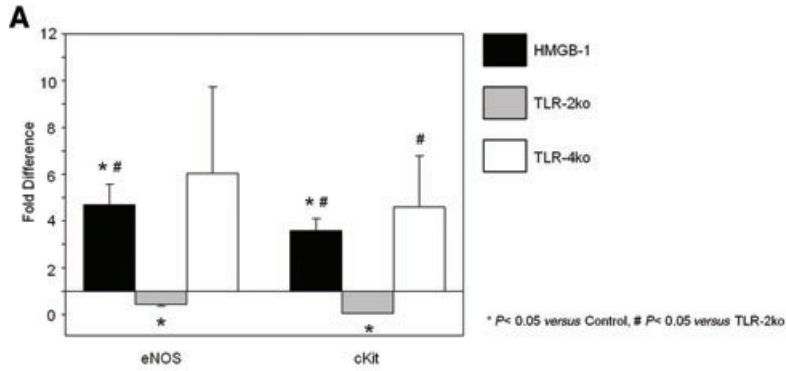
Fig. 3 HMGB-1 increases eNOS and c-kit expression in presence of TLR-2. Quantitative real-time PCR and confocal microscopy analysis of stem cell homing signals in cremaster muscle. (**A**) eNOS and c-kit genes expression in 'Control', 'HMGB-1', 'TLR-2ko' and 'TLR-4ko' groups. The average mRNA expression level of eNOS and c-kit in 'Control' cremaster muscle tissue was arbitrarily given a value of 1 (line) (*$P < 0.05$ *versus* 'Control', #$P < 0.05$ *versus* 'TLR-2ko'). (**B**) Representative confocal microscopic images illustrating different expression patterns of eNOS in 'HMGB-1' group. eNOS+ signals (green) were abundant at the endothelial lining (upper) and co-localized with adherent haematopoietic cells (lower). Red: TOPRO-3 in nuclei.

Stimulation with HMGB-1 induces β1-integrin, P-selectin and ICAM-1 polarization in mouse endothelial cells

To analyse the effect of HMGB-1 on the expression and redistribution of β1-integrin, P-selectin and ICAM-1 on endothelial plasmalemma, SVEC cells were preconditioned and observed by confocal microscopy. In HMGB-1–treated endothelial cells, we detected an evident polarization of membrane proteins compared to untreated controls (Fig. 6). HMGB-1 signal induced a prompt response of SVEC cells, which showed significant membrane redistribution of β1-integrin (10 ± 2 cells/HPF, $P < 0.05$), P-selectin (8 ± 4 cells/HPF, $P < 0.05$) and ICAM-1 (30 ± 4 cells/HPF, $P < 0.01$; Fig. 6). To clarify whether this effect is specific for HMGB-1, endothelial cells were additionally stimulated with SDF-1α and tumour necrosis factor alpha (TNF-α). Treatment with TNF-α, another well-known mediator of inflammation induced β1-integrin, P-selectin and ICAM-1 polarization in similar extent to HMGB-1 (Fig. 6). In contrast, pre-treatment of mouse

Fig. 4 The mRNA level of P-selectin in presence or absence of TLR-2 and TLR-4. Quantitative real-time PCR analysis in 'Control', 'HMGB-1', 'TLR-2ko' and 'TLR-4ko' groups. P-selectin mRNA is significantly up-regulated by HMGB-1 only when TLR-2 is functional. The average mRNA expression level of eNOS and c-kit in 'Control' cremasters was arbitrarily given a value of 1 (line) (**$P < 0.01$ *versus* 'Control').
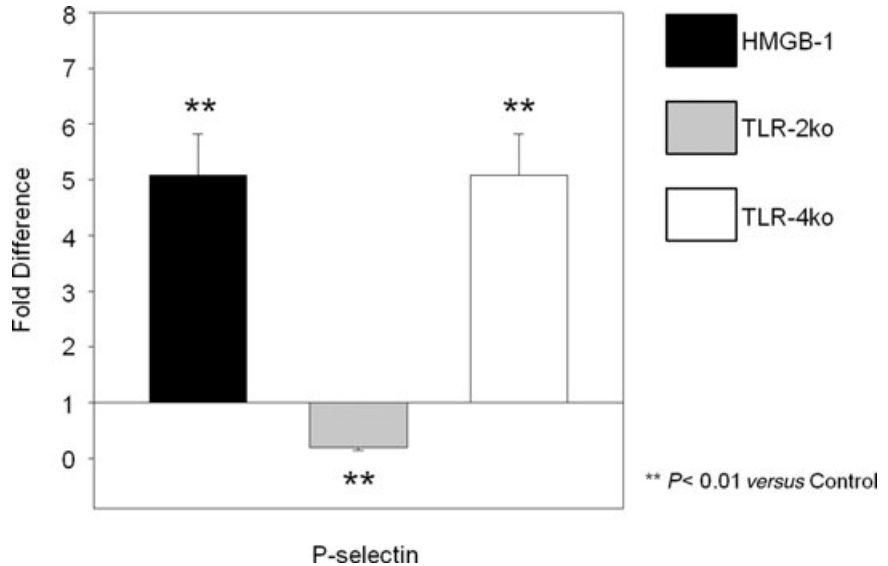
endothelial cells with SDF-1α–induced endothelial ICAM-1 but not β1-integrin and P-selectin polarization in a significant extent (Fig. 6).

Discussion

The primary intention of our study was to investigate the influence of HMGB-1, TLR-2 and TLR-4 on the preliminary phases of c-kit+ cell diapedesis and transmigration *in vivo*. In addition, we aimed to further characterize the effect of HMGB-1 on the expression of adhesion molecules, which are involved in cellular tethering, rolling and adhesion on the vascular wall *in vivo*. We describe for the first time the HMGB-1–dependent interactions of c-kit+ cells with the microvascular endothelium, using intravital microscopy. HMGB-1 preconditioning of mouse cremaster muscles triggered a significant increase in c-kit+ cell rolling and adhesion *in vivo*, which represent the first steps for cellular extravasation. Moreover, the chemokine generated a drastic up-regulation of eNOS and c-kit signals in the cremaster muscle after superfusion. The presence of both HMGB-1 receptors TLR-2 and TLR-4 on vascular endothelial cell was mandatory for HMGB-1–enhanced affinity between c-kit+ cells and the endothelial lining. Furthermore, TLR-2 was essential for the HMGB-1–mediated expression of eNOS, c-kit and P-selectin in the cremaster muscle after treatment. On the other hand, there was no difference of HMGB-1–mediated effects on c-kit+ isolated from TLR-2 (−/−) and Tlr4 (LPS-del) animals compared to 'control' cells. *In vitro*, HMGB-1 stimuli were determinant for the reorganization of important adhesion molecules on the plasmalemma of endothelial cells.

Our intravital microscopy study suggests that HMGB-1 is able to activate the cremaster endothelium immediately upon stimulation. The significantly increased rolling and adhesion behaviour of c-kit+ cells indicate that HMGB-1 could have an influence on the activation of endothelial signalling pathways, which may initiate the c-kit+ cell extravasation sequence. To our knowledge there are no other studies that focused on the direct intravital microscopic observation of HMGB-1–mediated c-kit+ cell interaction with the vascular endothelium. Few reports described intravital microscopy analysis of the murine bone marrow [17,18], while the majority of the studies in non-marrow organs have been performed on mature leukocyte behaviour [19,20]. Only a small number of records about peripheral stem cell–endothelium interactions *in vivo* are available [1,21,22]. In one of these, we illustrated that SDF-1α could significantly increase the adhesion capacity of c-kit+ cells only in presence of additional pro-inflammatory stimulus such as TNF-α [1]. Now, we demonstrate that HMGB-1 alone significantly increased c-kit+ cell commitment to roll and adhere on endothelial lining. This effect might corroborate the important inflammatory effect of HMGB-1 [3,6]. In fact, our current data show a minor increase of adherent ELs after HMGB-1 stimulation while it was not observed with SDF-1α in our previous study [1]. Our results support the view of HMGB-1 as a complex regulator of both inflammatory response and tissue regeneration.

The initiation of c-kit+ cell extravasation mediated by HMGB-1 was confirmed by the results of real-time PCR. Endothelial nitric oxide synthase, which has been shown to have a pivotal role in endothelial progenitor cells mobilization and homing [23, 24], was significantly up-regulated at mRNA and protein level. Moreover, the c-kit+ signal in the tissue was found to be considerably higher in 'HMGB-1' group compared to 'Control' detected by RT-PCR. These findings were agreeing with the c-kit+ cell homing potential
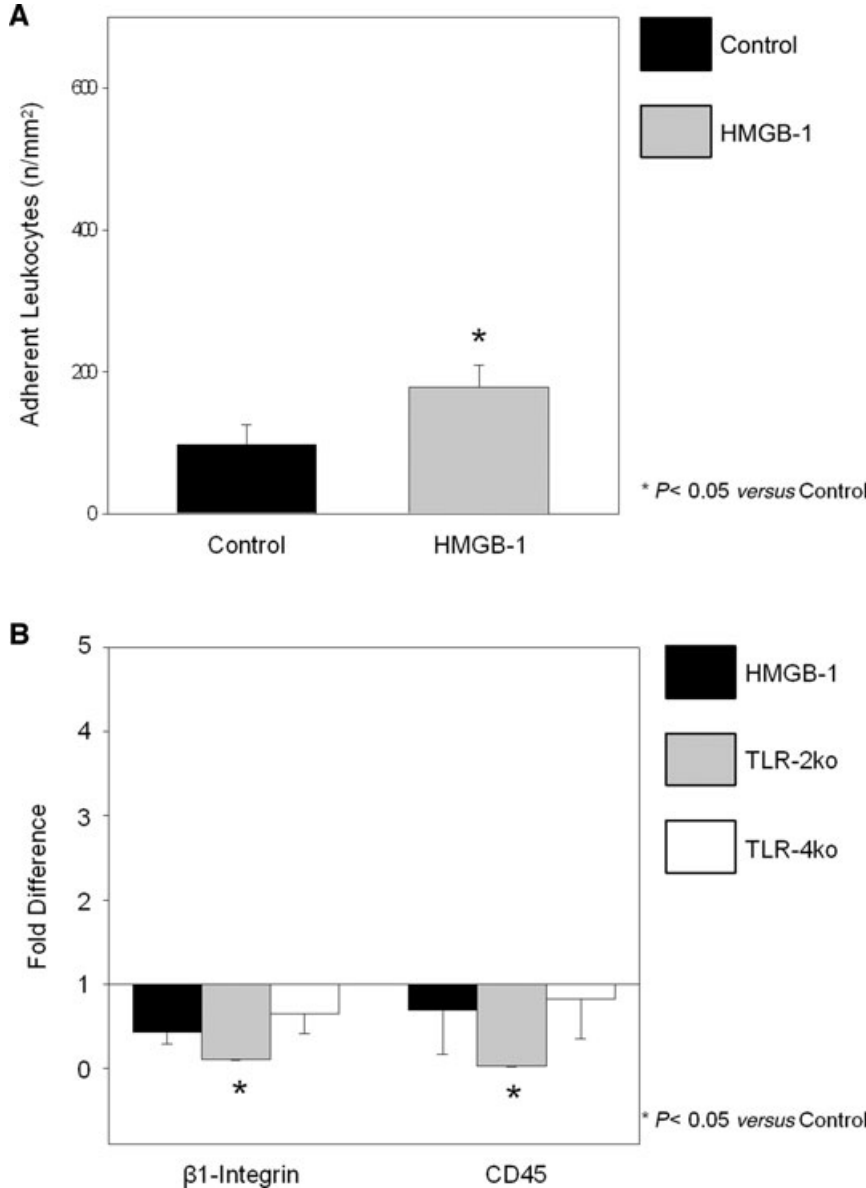
Fig. 5 Endogenous leukocyte adhesion on cremaster muscle 15 min. after direct HMGB-1 superfusion. (**A**) Number (n/mm^2) of adherent leukocytes in 'Control' and 'HMGB-1' groups. (**B**) Quantitative real-time PCR analysis of the pro-inflammatory signals β1-integrin and CD45 of 'Control', 'HMGB-1', 'TLR-2ko' and 'TLR-4ko' groups. The average mRNA expression level of β1-intergrin and CD45 and c-kit in 'Control' cremasters was arbitrarily given a value of 1 (line) (*$P < 0.05$ versus 'Control').

of HMGB-1 and suggest that its effect might be associated to eNOS activation.

Interestingly, we observed for the first time a central role of TLR-2 and TLR-4 on the rolling and adhesion ability of c-kit$^+$ cells. The depletion of TLR-2 and TLR-4 on the vascular endothelium abolished HMGB-1–induced c-kit$^+$ cell–endothelial interaction. However, there was no difference between c-kit$^+$ cells isolated from WT and TLR-2 (−/−) or Tlr4 (LPS-del) animals regarding their rolling and adhesion behaviour on the endothelium of WT animals. This data reveal a critical function of endothelial TLR-2

and TLR-4 on HMGB-1–mediated c-kit$^+$ cell migration. In addition, selective agonists of TLR-2 or TLR-4 alone were not capable to promote endothelial c-kit$^+$ cell adhesion, in the same manner as HMGB-1, indicating both receptors contribute to this effect. RT-PCR results suggest that TLR-2 mediates HMGB-1 effects on cellular adhesion *via* P- Selectin, whereas TLR-4 is likely to influence another adhesion molecule pattern such as VCAM-1 or ICAM-1. Moreover TLR-2 seems to stimulate HMGB-1–dependent moderate local inflammatory reaction, which has been shown to be crucial for c-kit$^+$ interaction with the endothelium [1]. With regard to

Fig. 6 HMGB-1–induced changes in the expression of SVEC surface adhesion molecules. (**A**) Representative immunofluorescent staining of β1-integrin in untreated and TNF-α, SDF-1α or HMGB-1–treated SVEC. (**B**) Number of SVEC showing β1-integrin polarization within the groups. (**C**) Representative images of P-selectin expression on SVEC plasmalemma in untreated and TNF-α, SDF-1α or HMGB-1–treated cells. (**D**) Number of SVEC showing P-selectin redistribution after stimulation with different cytokines. (**E**) Confocal images of ICAM-1 expression patterns on SVEC membrane. (**F**) Quantity of cells presenting ICAM-1 polarization after preconditioning with TNF-α, SDF-1α or HMGB-1 (*$P < 0.05$ *versus* 'Control'; **$P < 0.01$ *versus* 'Control', HPF = 630×).
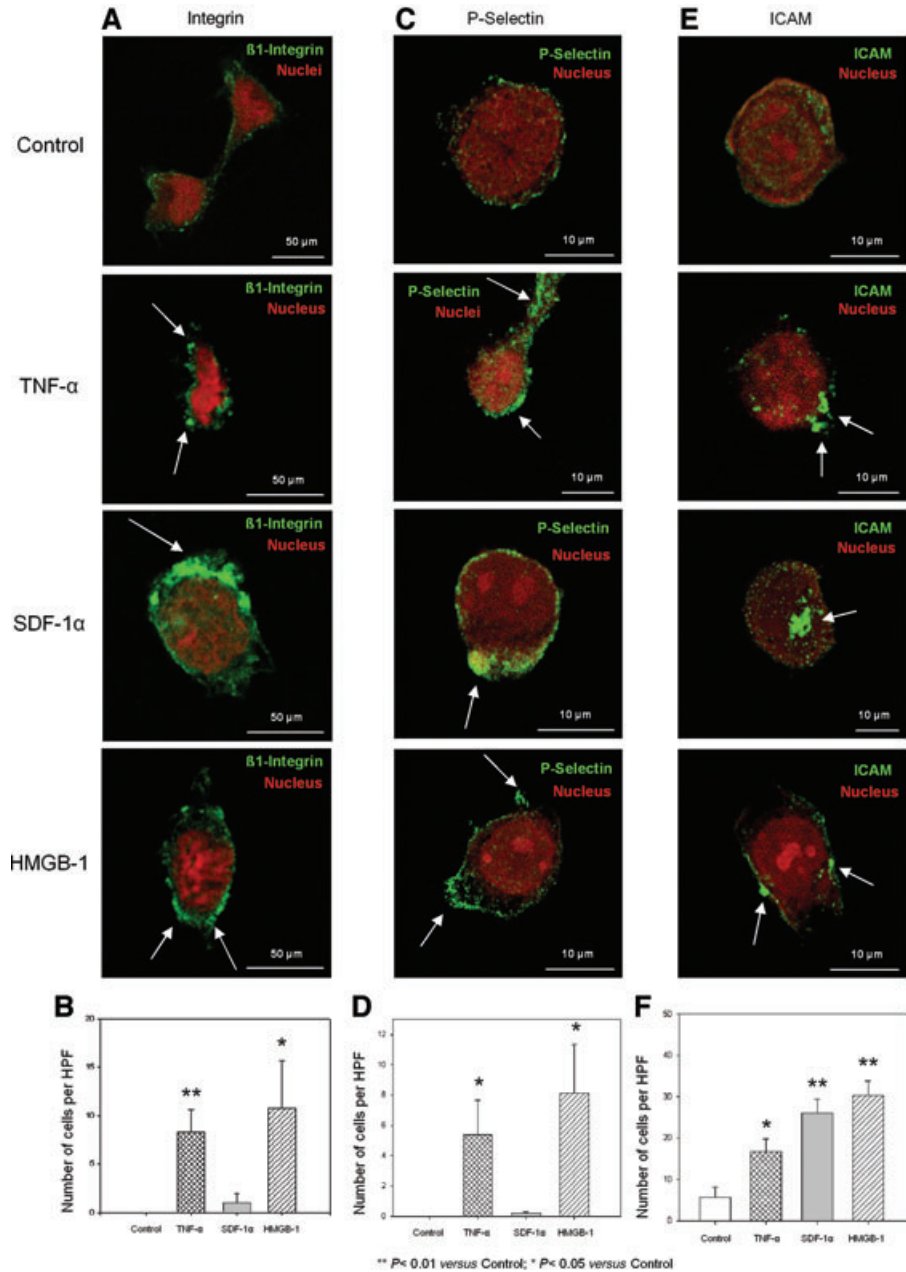
HMGB-1–mediated inflammation and stem cell mobilization, the exact role of HMGB-1 receptors TLR-2, TLR-4 and RAGE is still poorly understood. A previous study by Chavakis. [5] demonstrates the *in vitro* effects of HMGB-1 on human EPC adhesion and homing. They found that EPC expressed RAGE and TLR-2 but not TLR-4 on their surface. HMGB-1–induced EPC migration in a RAGE-dependent manner. Neutralizing TLR-2 did not influence the EPC migration significantly. In this study, we found that endothelial TLR-2 and TLR-4 signalling was mandatory for HMGB-1–mediated c-kit$^+$ cell recruitment. The discrepancy may be due to the fact that different cell populations may display distinct response mechanisms on stimulation with HMGB-1 [5]. van Zoelen *et al.* were able to show that an HMGB-1 associated increase of TNF-α, interleukin-6 and neutrophil numbers was dependent on TLR-4 and RAGE in the mouse [25]. On the other hand, the group of Yu described that there might be a differential usage of TLR-2 and TLR-4 in HMGB-1 signalling in primary cells or in cell lines [26].

In our investigation of HMGB-1 influence on adhesion molecule expression, we further displayed that the preconditioning of mouse endothelial cell line (SVEC) with HMGB-1 significantly affected the distribution of β1-integrin, P-selectin and ICAM-1 at the plasmalemma. The roles of β1-integrins in the recognition of extracellular matrix molecules has been extensively investigated [27–30]. Their several functions include the contribution to essential activities for the maintenance and functioning of blood vessels such as spreading, retraction, polarization and migration [31,32]. It is probable that the ability of HMGB-1 to reorganize β1-integrin on the endothelial membrane may be involved in the migration and extravasation of c-kit^{+} cells. In addition, HMGB-1 effect on the polarization of P-selectin and ICAM-1 in the endothelial cell line (SVEC) indicates that this chemokine could activate the endothelium eliciting c-kit[+] homing. The homing of c-kit^{+} cells to sites of neovascularization might share at least some common mechanisms with the homing of leukocytes to sites of inflammation.

An open question is still which other molecules are involved in the mechanisms of endothelial TLR-2 and TLR-4–dependent c-kit^{+} cells adhesion, rolling and penetration. HMGB-1 could activate a series of signalling components through TLR-2 and TLR-4. The activation of TLR-2 and TLR-4 through a MyD88-dependent mechanism may lead to nuclear factor-κB activation [33–35]. NF-κB, an important regulator of inflammation, could control the expression of genes encoding the pro-inflammatory cytokines and adhesion molecules (*e.g.* ICAM, VCAM, E-selectin) [33–35]. The up-regulation of adhesion molecules could increase adhesion of c-kit^{+} cells to stimulated endothelia and eventually promote cell recruitment. In addition, through binding of its receptor, HMGB1 elicited activation of metalloproteases 2 (MMP-2) and MMP-9 and enables the degradation of the extracellular matrix, which may further facilitate the cell penetration and migration [36].

The physiological relevance of HMGB-1 induced stem cell activation in the context of cardiovascular pathologies has been shown before by Limana *et al.* in an animal model of myocardial infarction. HMGB-1 was shown to induce myocardial regeneration after infarction by enhancement of c-kit[+] cell proliferation and differentiation [9]. Regarding the relevance of TLRs for stem cell based cardiovascular regeneration processes, recent evidence suggests that TLR-2 might be crucial for mesenchymal stem cell-associated myocardial recovery after ischaemia–reperfusion [37]. With respect of these results and the findings of Chavakis on HMGB-1–induced homing of endothelial progenitor cells [5], the further investigation of HMGB-1–dependent adhesion and migration of c-kit^{+} stem cells *in vivo,* as performed in the current project, seems conceivable. In addition, we speculated the co-treatment of LPS and MALP-2 may have the identical effect with HMGB-1. To clarify if the co-treatment is capable to mimic the effect of HMGB-1 *in vivo*, the further investigation should compare the effect of co-treatment with LPS and MALP-2 with HMGB-1.

In conclusion, we demonstrated that HMGB-1 might increase the migration of c-kit^{+} cells *in vivo* and activate the endothelial cells both *in vivo* and *in vitro*. These effects seem to be regulated through TLRs on endothelial but not on c-kit stem cell. Our study highlights the potential effect of HMGB-1 on enhancing stem cell recruitment for tissue regeneration and the essential function of its downstream signalling through TLRs.

Acknowledgements

Conflict of interest

The authors confirm that there are no known conflicts of interest associated with this publication.

Supporting Information

Additional Supporting Information may be found in the online version of this article:

Fig. S1 FACS analysis of murine bone marrow derived c-kit[+] cell from WT, TLR-2 (−/−) and Tlr4 (LPS-del) for purity and surface molecule expression.

Table S1 Primers used in real-time PCR

Table S2 Microvascular haemodynamics of murine cremaster muscle

Please note: Wiley-Blackwell is not responsible for the content or functionality of any supporting materials supplied by the authors. Any queries (other than missing material) should be directed to the corresponding author for the article.

References

1. **Kaminski A, Ma N, Donndorf P, *et al.*** Endothelial NOS is required for SDF-1alpha/CXCR4-mediated peripheral endothelial adhesion of c-kit+ bone marrow stem cells. *Lab Invest.* 2008; 88: 58–69.

2. **Bianchi ME, Manfredi A.** Chromatin and cell death. *Biochim Biophys Acta.* 2004; 1677: 181–6.

3. **Palumbo R, Galvez BG, Pusterla T, *et al.*** Cells migrating to sites of tissue damage in response to the danger signal HMGB1 require NF-kappaB activation. *The Journal of cell biology.* 2007; 179: 33–40.

4. **Palumbo R, Bianchi ME.** High mobility group box 1 protein, a cue for stem cell recruitment. *Biochem Pharmacol.* 2004; 68: 1165–70.

5. **Chavakis E, Hain A, Vinci M, *et al.*** High-mobility group box 1 activates integrin-dependent homing of endothelial progenitor cells. *Circulat Res.* 2007; 100: 204–12.

6. **Palumbo R, Sampaolesi M, De Marchis F, *et al.*** Extracellular HMGB1, a signal of tissue damage, induces mesoangioblast migration and proliferation. *J Cell Biol.* 2004; 164: 441–9.

7. **Fiuza C, Bustin M, Talwar S, *et al.*** Inflammation-promoting activity of HMGB1 on human microvascular endothelial cells. *Blood.* 2003; 101: 2652–60.

8. **Urbich C, Dimmeler S.** Endothelial progenitor cells: characterization and role in vascular biology. *Circulat Res.* 2004; 95: 343–53.

9. **Limana F, Germani A, Zacheo A, *et al.*** Exogenous high-mobility group box 1 protein induces myocardial regeneration after infarction *via* enhanced cardiac C-kit+ cell proliferation and differentiation. *Circulation research.* 2005; 97: e73–83.

10. **Kabrun N, Buhring HJ, Choi K, *et al.*** Flk-1 expression defines a population of early embryonic hematopoietic precursors. *Development.* 1997; 124: 2039–48.

11. **Rafii S, Lyden D.** Therapeutic stem and progenitor cell transplantation for organ vascularization and regeneration. *Nat Med.* 2003; 9: 702–12.

12. **Fazel S, Cimini M, Chen L, *et al.*** Cardioprotective c-kit+ cells are from the bone marrow and regulate the myocardial balance of angiogenic cytokines. *J Clin Invest.* 2006; 116: 1865–77.

13. **Rossini A, Zacheo A, Mocini D, *et al.*** HMGB1-stimulated human primary cardiac fibroblasts exert a paracrine action on human and murine cardiac stem cells. *J Mol Cell Cardiol.* 2008; 44: 683–93.

14. **Baker M, Wayland H.** On-line volume flow rate and velocity profile measurement for blood in microvessels. *Microvasc Res.* 1974; 7: 131–43.

15. **Baez S.** An open cremaster muscle preparation for the study of blood vessels by *in vivo* microscopy. *Microvasc Res.* 1973; 5: 384–94.

16. **Vollmar B, Schmits R, Kunz D, *et al.*** Lack of *in vivo* function of CD31 in vascular thrombosis. *Thromb Haemost.* 2001; 85: 160–4.

17. **Frenette PS, Subbarao S, Mazo IB, *et al.*** Endothelial selectins and vascular cell adhesion molecule-1 promote hematopoietic progenitor homing to bone marrow. *Proc Natl Acad Sci USA.* 1998; 95: 14423–8.

18. **Mazo IB, Gutierrez-Ramos JC, Frenette PS, *et al.*** Hematopoietic progenitor cell rolling in bone marrow microvessels: parallel contributions by endothelial selectins and vascular cell adhesion molecule 1. *J Exp Med.* 1998; 188: 465–74.

19. **Thorlacius H, Vollmar B, Guo Y, *et al.*** Lymphocyte function antigen 1 (LFA-1) mediates early tumour necrosis factor alpha-induced leucocyte adhesion in venules. *Br J Haematol.* 2000; 110: 424–9.

20. **Zarbock A, Ley K.** New insights into leukocyte recruitment by intravital microscopy. *Curr Top Microbiol Immunol.* 2009; 334: 129–52.

21. **Ruster B, Gottig S, Ludwig RJ, *et al.*** Mesenchymal stem cells display coordinated rolling and adhesion behavior on endothelial cells. *Blood.* 2006; 108: 3938–44.

22. **Furlani D, Ugurlucan M, Ong L, *et al.*** Is the intravascular administration of mesenchymal stem cells safe? Mesenchymal stem cells and intravital microscopy. *Microvasc Res.* 2009; 77: 370–6.

23. **Klopsch C, Furlani D, Gabel R, *et al.*** Intracardiac injection of erythropoietin induces stem cell recruitment and improves cardiac functions in a rat myocardial infarction model. *J Cell Mol Med.* 2009; 13: 664–79.

24. **Wegiel B, Gallo DJ, Raman KG, *et al.*** Nitric oxide-dependent bone marrow progenitor mobilization by carbon monoxide enhances endothelial repair after vascular injury. *Circulation.* 121: 537–48.

25. **van Zoelen MA, Yang H, Florquin S, *et al.*** Role of toll-like receptors 2 and 4, and the receptor for advanced glycation end products in high-mobility group box 1-induced inflammation *in vivo*. *Shock.* 2009; 31: 280–4.

26. **Yu M, Wang H, Ding A, *et al.*** HMGB1 signals through toll-like receptor (TLR) 4 and TLR2. *Shock.* 2006; 26: 174–9.

27. **Smith CW.** Endothelial adhesion molecules and their role in inflammation. *Can J Physiol Pharmacol.* 1993; 71: 76–87.

28. **Ridley AJ, Schwartz MA, Burridge K, *et al.*** Cell migration: integrating signals from front to back. *Science.* 2003; 302: 1704–9.

29. **Clark EA, Brugge JS.** Integrins and signal transduction pathways: the road taken. *Science.* 1995; 268: 233–9.

30. **Sobel RA, Hinojoza JR, Maeda A, *et al.*** Endothelial cell integrin laminin receptor expression in multiple sclerosis lesions. *Am J Pathol.* 1998; 153: 405–15.

31. **Dejana E, Raiteri M, Resnati M, *et al.*** Endothelial integrins and their role in maintaining the integrity of the vessel wall. *Kidney Int.* 1993; 43: 61–5.

32. **Shattil SJ, Ginsberg MH.** Perspectives series: cell adhesion in vascular biology. Integrin signaling in vascular biology. *J Clin Invest.* 1997; 100: 1–5.

33. **Ellerman JE, Brown CK, de Vera M, *et al.*** Masquerader: high mobility group box-1 and cancer. *Clin Cancer Res.* 2007; 13: 2836–48.

34. **Lotze MT, Tracey KJ.** High-mobility group box 1 protein (HMGB1): nuclear weapon in the immune arsenal. *Nat Rev Immunol.* 2005; 5: 331–42.

35. **Vakkila J, Lotze MT.** Inflammation and necrosis promote tumour growth. *Nat Rev Immunol.* 2004; 4: 641–8.

36. **Muller S, Scaffidi P, Degryse B, *et al.*** New EMBO members' review: the double life of HMGB1 chromatin protein: architectural factor and extracellular signal. *EMBO J.* 2001; 20: 4337–40.

37. **Abarbanell AM, Wang Y, Herrmann JL, *et al.*** Toll-like receptor 2 mediates mesenchymal stem cell-associated myocardial recovery and VEGF production following acute ischaemia-reperfusion injury. *Am J Physiol Heart Circ Physiol.* 298: H1529–36.